Available online at www.sciencedirect.com

ScienceDirect

Physics Procedia 1 (2008) 257–264

Physics Procedia

www.elsevier.com/locate/procedia

Proceedings of the Seventh International Conference on Charged Particle Optics

Calculation of fields of magnetic deflection systems with FEM using a vector potential approach - Part II: time-dependent fields

T. Elster*, D. Stahl and P. Hahmann

Vistec Electron Beam GmbH, Göschwitzer Straße 25, 07745 Jena, Germany

Received 9 July 2008; received in revised form 9 July 2008; accepted 9 July 2008

Abstract

A procedure is presented for calculating time-dependent fields in magnetic deflection systems (especially saddle coils) in a rotationally symmetric surrounding consisting of materials with arbitrary permeability and conductivity using the FEM method and a vector potential approach. The vector potential and the current distribution are expanded as Fourier series with respect to the azimuthal coordinate φ. Consequently, each harmonic can be handled as a separate two-dimensional problem. The backward Euler method is used for time integration. Corrections of the local FEM equations are calculated which originate from the time dependence. The global FEM equations coincide with the corresponding equations in the stationary case.

PACS: 41.85.-p; 81.70.Ex; 47.11.Fg

Keywords: Electron optics; Deflection system; Eddy current; Settling time; Finite element method

1. Introduction

Magnetic deflection systems are used in devices such as electron beam lithography systems. The time-dependent field of these deflectors creates eddy currents in conducting materials such as pole pieces of lenses. The settling time of these deflectors, which is caused by eddy currents, is of particular interest since it influences throughput.

Time-dependent three-dimensional field approaches with the magnetic vector potential have been described elsewhere [4], and commercially available FEM software can be used to simulate three-dimensional eddy current effects. However, the fully three-dimensional approach is very time-consuming and requires a large amount of computer resources. In the specific case of a deflector in a complicated magnetic lens surrounding with shielding ferrites etc. the three-dimensional approach is nearly impossible.

In a first paper of this series [1] a vector potential approach was presented to calculate stationary fields of magnetic deflection systems in ferromagnetic surroundings using the Finite Element Method (FEM). Although this

* Corresponding author. Tel.: +49-3641-651932
E-mail address: thomas.elster@vistec-semi.com

doi:10.1016/j.phpro.2008.07.104

approach is also useful for the computation of stationary fields, the actual reason for using the vector potential was the application to time-dependent fields. The magnetic scalar potential approach ([2], [3]) suitable for calculating stationary fields can no longer be employed for time-dependent fields because eddy currents are created in conducting materials and $curl\,\vec{H}$ is no longer zero in eddy current regions. Therefore, in the time-dependent case, the vector potential has to be used throughout.

In this paper we are focussing on the time-dependent fields of saddle coils. However, the case of toroidal coils can be handled similarly. Fortunately, in electron optics only few field harmonics are of interest and therefore the three-dimensional problem can be replaced by few two-dimensional problems.

Since both the magnetic vector potential $\vec{a}$ and the current distribution $\vec{j}$ are expanded into Fourier series with respect to the azimuth angle φ of the cylindrical coordinate system, each Fourier harmonic of $\vec{a}$ can be handled as a separate two-dimensional FEM problem. Therefore only few two-dimensional FEM problems have to be solved instead of a much more complicated three-dimensional FEM problem as long as the distribution of ferromagnetic and/or conducting materials is rotationally symmetric (see [2], [3] for the magnetic scalar potential case).

2. Energy functional for the vector potential formulation

The Maxwell equations for a time-dependent magnetic field are

$$\begin{aligned} curl\,\vec{H} &= \vec{j} + \frac{\partial \vec{D}}{\partial t} \\ curl\,\vec{E} &= -\frac{\partial \vec{B}}{\partial t} \\ div\,\vec{B} &= 0 \\ div\,\vec{D} &= \rho \end{aligned} \tag{1}$$

together with the material equation

$$\vec{B} = \mu_0 \mu_r \vec{H}. \tag{2}$$

As usual in the quasi-stationary approximation the displacement current is neglected ($\partial \vec{D} / \partial t = 0$). Moreover, we assume that there are no free charges ($\rho = 0$). The current density can be written as

$$\vec{j} = \vec{j}_0 + \vec{j}_e \tag{3}$$

where $\vec{j}_0$ is the specified current density in the coils, and $\vec{j}_e$ is the eddy current density induced in conductors by changing magnetic fields. The latter is given by

$$\vec{j}_e = \sigma \cdot \vec{E} \tag{4}$$

where σ is the electric conductivity.

The third of equation (1) is satisfied with the ansatz

$$\vec{B} = curl\,\vec{a}, \tag{5}$$

where $\vec{a}$ is the magnetic vector potential. Inserting (5) in (1b) gives:

$$\vec{E} = -\frac{\partial \vec{a}}{\partial t} \tag{6}$$

From (4) and (6) we get:

$$\vec{j}_e = -\sigma \frac{\partial \vec{a}}{\partial t}. \tag{7}$$

Using (1a), (2), (5) and (7) we get the diffusion equation:

$$curl\left(\frac{1}{\mu_0\mu_r} curl\ \vec{a}\right) + \sigma \cdot \frac{\partial \vec{a}}{\partial t} = \vec{j}_0. \tag{8}$$

Equation (8) can be derived as Euler-Lagrange equation from an energy functional

$$W = \int £ \mathrm{dV} \tag{9}$$

containing the Lagrange density

$$£ = -\frac{1}{2\mu_0\mu_r}\left(curl\ \vec{a}\right)^2 - \frac{1}{2}\cdot\sigma\frac{\partial \vec{a}}{\partial t}\vec{a} + \vec{j}_0\vec{a}. \tag{10}$$

3. Time integration procedure

In a first step for time integration we employ the backward Euler method ([5], [6]). Let t_n be the sequence of time integration points and $h = t_n - t_{n-1}$ the time step size. The magnetic vector potential $\vec{a}(t_n)$ at the time t_n can be written as:

$$\vec{a}(t_n) = \vec{a}(t_{n-1}) + h \cdot \left(\frac{\partial \vec{a}}{\partial t}\right)_{t=t_n} \tag{11}$$

Solving (11) for $\left(\partial\vec{a}/\partial t\right)_{t=t_n}$ and using (8) gives the time-discretized diffusion equation:

$$curl\left(\frac{1}{\mu_0\mu_r} curl\ \vec{a}(t_n)\right) + \frac{\sigma}{h}\cdot\left[\vec{a}(t_n) - \vec{a}(t_{n-1})\right] = \vec{j}_0(t_n). \tag{12}$$

Equation (12) is a purely "space-like" differential equation (i.e. it contains only spatial derivatives with respect to the coordinates (r, φ, z)) for the vector potential $\vec{a}(t_n)$ at the time t_n provided that the vector potential $\vec{a}(t_{n-1})$ at the time t_{n-1} is already known. The Lagrange density now takes the form:

$$£ = -\frac{1}{2\mu_0\mu_r}\left(curl\ \vec{a}(t_n)\right)^2 - \frac{1}{2h}\cdot\sigma\cdot\left[\vec{a}(t_n) - \vec{a}(t_{n-1})\right]\cdot\vec{a}(t_n) + \vec{j}_0(t_n)\cdot\vec{a}(t_n) \tag{13}$$

In the following we use cylindrical coordinates (r, φ, z). In these coordinates (13) can be written as:

$$\begin{aligned} £ = &-\frac{1}{2\mu_0\mu_r}\left[\left(\frac{1}{r}\frac{\partial a_z(t_n)}{\partial\varphi} - \frac{\partial a_\varphi(t_n)}{\partial z}\right)^2 + \left(\frac{\partial a_r(t_n)}{\partial z} - \frac{\partial a_z(t_n)}{\partial r}\right)^2 + \frac{1}{r^2}\left(r\frac{\partial a_\varphi(t_n)}{\partial r} + a_\varphi(t_n) - \frac{\partial a_r(t_n)}{\partial\varphi}\right)^2\right] \\ &-\frac{\sigma}{2h}\cdot\left[\left(a_r(t_n) - a_r(t_{n-1})\right)\cdot a_r(t_n) + \left(a_\varphi(t_n) - a_\varphi(t_{n-1})\right)\cdot a_\varphi(t_n) + \left(a_z(t_n) - a_z(t_{n-1})\right)\cdot a_z(t_n)\right] \\ &+\left(j_r(t_n)\cdot a_r(t_n) + j_\varphi(t_n)\cdot a_\varphi(t_n) + j_z(t_n)\cdot a_z(t_n)\right) \end{aligned} \tag{14}$$

We now expand the components of the vector potential in Fourier series of mth harmonics in the azimuthal coordinate φ, i.e.

$$a_\alpha(r,\varphi,z,t) = \sum_{m=1,3,5...}\left[a_\alpha^m(r,z,t)\cdot\cos(m\varphi) + b_\alpha^m(r,z,t)\cdot\sin(m\varphi)\right], \tag{15}$$

where Greek indices $\alpha, \beta, \gamma, ... = 0,1,2$ are running through the coordinates (r, φ, z) throughout the paper. In the case of ideal deflection systems only odd Fourier harmonics contribute to the expansion (15).

In the following, we confine ourselves to the case of magnetic saddle coils, although the treatment of toroidal coils can be handled similarly. As shown by Munro and Chu [2] and Lencova et al [3] the current density $\vec{j} = (j_r, j_\varphi, j_z)$ of a saddle coil can be derived from a single function $F_r(r,\varphi,z)$, which is non-vanishing only inside the coil windings, i.e.

$$j_r = 0 \qquad j_\varphi = \frac{\partial F_r}{\partial z} \qquad j_z = -\frac{1}{r}\cdot\frac{\partial F_r}{\partial \varphi}. \tag{16}$$

It is now straightforward to follow the procedure outlined in our first paper of this series [1] to derive the energy functional W^m of the m^{th} harmonic.

Integrating over φ and using the orthonormalization relations of the trigonometric functions we finally obtain the expression

$$W^m = -\frac{\pi^2}{2}\cdot\int\frac{1}{\mu_0\mu_r}\cdot\left\{\begin{array}{l} \left(\frac{m}{r}a_2^m(t_n)+\frac{\partial b_1^m(t_n)}{\partial z}\right)^2+\left(\frac{m}{r}b_2^m(t_n)-\frac{\partial a_1^m(t_n)}{\partial z}\right)^2+\left(\frac{\partial a_0^m(t_n)}{\partial z}-\frac{\partial a_2^m(t_n)}{\partial r}\right)^2 \\ +\left(\frac{\partial b_0^m(t_n)}{\partial z}-\frac{\partial b_2^m(t_n)}{\partial r}\right)^2 \\ +\left(\frac{\partial a_1^m(t_n)}{\partial r}+\frac{1}{r}\cdot a_1^m(t_n)-\frac{m}{r}b_0^m(t_n)\right)^2+\left(\frac{\partial b_1^m(t_n)}{\partial r}+\frac{1}{r}\cdot b_1^m(t_n)+\frac{m}{r}a_0^m(t_n)\right)^2 \\ +\frac{\mu_0\mu_r\sigma}{h}\cdot\left[\begin{array}{l}\left(a_0^m(t_n)-a_0^m(t_{n-1})\right)\cdot a_0^m(t_n)+\left(a_1^m(t_n)-a_1^m(t_{n-1})\right)\cdot a_1^m(t_n) \\ +\left(a_2^m(t_n)-a_2^m(t_{n-1})\right)\cdot a_2^m(t_n)\end{array}\right] \\ -2\,\mu_0\mu_r\frac{\partial g}{\partial z}f_m a_1^m(t_n)-2\mu_0\mu_r\frac{1}{r}g f_m b_2^m(t_n) \end{array}\right\} rdrdz \tag{17}$$

where the range of integration extends over the whole region in the r-z-plane considered. The last but one term in the braces can be rewritten by using integration by parts. The definition of the function $g(r,z)$ and the coefficients f_m are given in [1]. The coefficients f_m contain the current I inside the coil, the wire thickness ΔR and the semi-angle Θ of the saddle winding.

4. Discretization of the r-z plane and local FEM equations

We utilize the first order FEM method (FOFEM) and subdivide the region in the r-z-plane into quadrilaterals. Each quadrilateral is subdivided into a *left upper triangle* and *right lower triangle*, see Fig. 1 in [1]. The quadrilaterals are numbered by $ii = 0 \ldots nez-2$, $jj = 0 \ldots ner-2$, where nez is the number of mesh points in z direction and ner is the number of mesh points in r direction.

We denote by $\Delta W^{m,ii,jj,lower}$ the approximate expression of the energy functional of the m^{th} Fourier harmonic integrated over the right lower triangle of the quadrilateral (ii, jj). (For a left upper triangle the energy functional is $\Delta W^{m,ii,jj,upper}$.)

It is now again straightforward to follow the discretization procedure outlined in [1] to derive the approximate expression for the energy functional integrated over the right lower triangle of the quadrilateral

$$\Delta W^{m,ii,jj,lower} = -\frac{\pi^2}{2}\cdot|D|\cdot r_c\cdot\left\{\begin{array}{l} stationary\ terms\ at\ time\ t_n \\ +\frac{\sigma}{2h}\cdot\left[\begin{array}{l}\left(\frac{1}{3}\sum_{i=0}^{2}a_{0,i}^{m}(t_n)-\frac{1}{3}\sum_{i=0}^{2}a_{0,i}^{m}(t_{n-1})\right)\cdot\frac{1}{3}\sum_{i=0}^{2}a_{0,i}^{m}(t_n)\\ +\left(\frac{1}{3}\sum_{i=0}^{2}a_{1,i}^{m}(t_n)-\frac{1}{3}\sum_{i=0}^{2}a_{1,i}^{m}(t_{n-1})\right)\cdot\frac{1}{3}\sum_{i=0}^{2}a_{1,i}^{m}(t_n)\\ +\left(\frac{1}{3}\sum_{i=0}^{2}a_{2,i}^{m}(t_n)-\frac{1}{3}\sum_{i=0}^{2}a_{2,i}^{m}(t_{n-1})\right)\cdot\frac{1}{3}\sum_{i=0}^{2}a_{2,i}^{m}(t_n)\\ +\left(\frac{1}{3}\sum_{i=0}^{2}b_{0,i}^{m}(t_n)-\frac{1}{3}\sum_{i=0}^{2}b_{0,i}^{m}(t_{n-1})\right)\cdot\frac{1}{3}\sum_{i=0}^{2}b_{0,i}^{m}(t_n)\\ +\left(\frac{1}{3}\sum_{i=0}^{2}b_{1,i}^{m}(t_n)-\frac{1}{3}\sum_{i=0}^{2}b_{1,i}^{m}(t_{n-1})\right)\cdot\frac{1}{3}\sum_{i=0}^{2}b_{1,i}^{m}(t_n)\\ +\left(\frac{1}{3}\sum_{i=0}^{2}b_{2,i}^{m}(t_n)-\frac{1}{3}\sum_{i=0}^{2}b_{2,i}^{m}(t_{n-1})\right)\cdot\frac{1}{3}\sum_{i=0}^{2}b_{2,i}^{m}(t_n)\end{array}\right]\end{array}\right\} \tag{18}$$

(similarly for the left upper triangle), where "stationary terms at time t_n" denotes the terms already determined for the stationary case [1] taken at time t_n. The $a_{\alpha,i}^{m}(t_n)$ and $b_{\alpha,i}^{m}(t_n)$ are the values of the components of the vector potential of the m^{th} harmonic in the i^{th} point (node) (i=0…2) of the triangle considered.

The calculation of the local FEM equations follows the procedure described in [1]. The local FEM equations stating how the value of $\Delta W^{m,ii,jj,lower}$ changes if the potential at the corners of the triangles changes are

$$\begin{aligned}\frac{\partial\Delta W^{m,ii,jj,lower}}{\partial a_{\alpha,i}^{m}(t_n)} &= \sum_{\beta=0}^{2}\sum_{j=0}^{2}F_{\alpha,\beta,i,j}^{m,ii,jj,lower}\cdot a_{\beta,j}^{m}+\sum_{\beta=0}^{2}\sum_{j=0}^{2}H_{\alpha,\beta,i,j}^{m,ii,jj,lower}\cdot b_{\beta,j}^{m}+G_{\alpha,i}^{m,ii,jj,lower}\\ \frac{\partial\Delta W^{m,ii,jj,lower}}{\partial b_{\alpha,i}^{m}(t_n)} &= \sum_{\beta=0}^{2}\sum_{j}^{2}R_{\alpha,\beta,i,j}^{m,ii,jj,lower}\cdot a_{\beta,j}^{m}+\sum_{\beta=0}^{2}\sum_{j=0}^{2}S_{\alpha,\beta,i,j}^{m,ii,jj,lower}\cdot b_{\beta,j}^{m}+T_{\alpha,i}^{m,ii,jj,lower}\end{aligned} \tag{19}$$

(similarly for the left upper triangles). The coefficients are given by

$$\begin{aligned}F_{0,0,i,j}^{m,ii,jj,lower} &= stationary\ terms-\frac{\pi^2}{2}|D|\cdot r_c\cdot\frac{\sigma}{9h}\\ F_{1,1,i,j}^{m,ii,jj,lower} &= stationary\ terms-\frac{\pi^2}{2}|D|\cdot r_c\cdot\frac{\sigma}{9h}\\ F_{2,2,i,j}^{m,ii,jj,lower} &= stationary\ terms-\frac{\pi^2}{2}|D|\cdot r_c\cdot\frac{\sigma}{9h}\\ S_{0,0,i,j}^{m,ii,jj,lower} &= stationary\ terms-\frac{\pi^2}{2}|D|\cdot r_c\cdot\frac{\sigma}{9h}\\ S_{1,1,i,j}^{m,ii,jj,lower} &= stationary\ terms-\frac{\pi^2}{2}|D|\cdot r_c\cdot\frac{\sigma}{9h}\\ S_{2,2,i,j}^{m,ii,jj,lower} &= stationary\ terms-\frac{\pi^2}{2}|D|\cdot r_c\cdot\frac{\sigma}{9h}\end{aligned} \tag{20a}$$

(all other $F_{\alpha,\beta,i,j}^{m,ii,jj,lower}, H_{\alpha,\beta,i,j}^{m,ii,jj,lower}, R_{\alpha,\beta,i,j}^{m,ii,jj,lower}, S_{\alpha,\beta,i,j}^{m,ii,jj,lower}$ remain unchanged compared with the stationary case) and

$$\begin{aligned}
G_{0,i}^{m,ii,jj,lower} &= stationary\ terms + \frac{\pi^2}{2}|D| \cdot r_c \cdot \frac{\sigma}{18h} \cdot \sum_{j=0}^{2} a_{0,j}^{m}(t_{n-1}) \\
G_{1,i}^{m,ii,jj,lower} &= stationary\ terms + \frac{\pi^2}{2}|D| \cdot r_c \cdot \frac{\sigma}{18h} \cdot \sum_{j=0}^{2} a_{1,j}^{m}(t_{n-1}) \\
G_{2,i}^{m,,ii,jj,lower} &= stationary\ terms + \frac{\pi^2}{2}|D| \cdot r_c \cdot \frac{\sigma}{18h} \cdot \sum_{j=0}^{2} a_{2,j}^{m}(t_{n-1}) \\
T_{0,i}^{m,ii,jj,lower} &= stationary\ terms + \frac{\pi^2}{2}|D| \cdot r_c \cdot \frac{\sigma}{18h} \cdot \sum_{j=0}^{2} b_{0,j}^{m}(t_{n-1}) \\
T_{1,i}^{m,ii,jj,lower} &= stationary\ terms + \frac{\pi^2}{2}|D| \cdot r_c \cdot \frac{\sigma}{18h} \cdot \sum_{j=0}^{2} b_{1,j}^{m}(t_{n-1}) \\
T_{2,i}^{m,ii,jj,lower} &= stationary\ terms + \frac{\pi^2}{2}|D| \cdot r_c \cdot \frac{\sigma}{18h} \cdot \sum_{j=0}^{2} b_{2,j}^{m}(t_{n-1})
\end{aligned} \tag{20b}$$

(similarly for the left upper triangles). “Stationary terms” means that we have to insert here the terms already calculated in [1] for the stationary field. The local FEM equations (20 a, b) are the basis for the FEM software. Obviously, the local FEM coefficients have the symmetry (as in the stationary case):

$$\begin{aligned}
F_{\alpha,\beta,i,j}^{m,ii,jj,lower} &= F_{\beta,\alpha,j,i}^{m,ii,jj,lower} \\
H_{\alpha,\beta,i,j}^{m,ii,jj,lower} &= -H_{\beta,\alpha,j,i}^{m,ii,jj,lower} \\
R_{\alpha,\beta,i,j}^{m,ii,jj,lower} &= -R_{\beta,\alpha,j,i}^{m,ii,jj,lower} \\
S_{\alpha,\beta,i,j}^{m,ii,jj,lower} &= S_{\beta,\alpha,j,i}^{m,ii,jj,lower}
\end{aligned} \tag{21}$$

This is important, because it causes the matrix of the global FEM system of equations to be symmetric (see next section). Here $|D|$ is twice the area of the triangle,

$$D = b_0 c_1 - b_1 c_0 = b_1 c_2 - b_2 c_1 = b_2 c_0 - b_0 c_2, \tag{22}$$

and b_i, c_i are the coordinate differences

$$\begin{aligned}
b_0 &= r_1 - r_2 \qquad b_1 = r_2 - r_0 \qquad b_2 = r_0 - r_1 \\
c_0 &= z_2 - z_1 \qquad c_1 = z_0 - z_2 \qquad c_2 = z_1 - z_0,
\end{aligned} \tag{23}$$

and (r_0, z_0), (r_1, z_1) and (r_2, z_2) are the coordinates of the corners of the triangle. (r_c, z_c) denotes the coordinates of the centroid of the triangle.

5. Global FEM System of Equations

The Maxwell equations are fulfilled if the energy functional is minimized. This leads to a linear system of equations for the unknowns. These equations can be written as

$$\begin{aligned}
&\left(\frac{\partial \Delta W^m}{\partial a_{\alpha,p}^m}\right)_{E1} + \left(\frac{\partial \Delta W^m}{\partial a_{\alpha,p}^m}\right)_{E2} + \left(\frac{\partial \Delta W^m}{\partial a_{\alpha,p}^m}\right)_{E3} + \left(\frac{\partial \Delta W^m}{\partial a_{\alpha,p}^m}\right)_{E4} + \left(\frac{\partial \Delta W^m}{\partial a_{\alpha,p}^m}\right)_{E5} + \left(\frac{\partial \Delta W^m}{\partial a_{\alpha,p}^m}\right)_{E6} = 0 \\
&\left(\frac{\partial \Delta W^m}{\partial b_{\alpha,p}^m}\right)_{E1} + \left(\frac{\partial \Delta W^m}{\partial b_{\alpha,p}^m}\right)_{E2} + \left(\frac{\partial \Delta W^m}{\partial b_{\alpha,p}^m}\right)_{E3} + \left(\frac{\partial \Delta W^m}{\partial b_{\alpha,p}^m}\right)_{E4} + \left(\frac{\partial \Delta W^m}{\partial b_{\alpha,p}^m}\right)_{E5} + \left(\frac{\partial \Delta W^m}{\partial b_{\alpha,p}^m}\right)_{E6} = 0
\end{aligned} \tag{24}$$

where p denotes a point in the finite element mesh, see Fig.1 in [1], and the ΔW^m are the energy functionals of the adjacent triangles *E1*…*E6* of *p*.

The potential components $a^m_{\alpha,i}$ and $b^m_{\alpha,i}$ ($\alpha = 0\ldots2$, $i = 0\ldots nez{*}ner-1$) are arranged in the solution vector as follows:

$$\begin{pmatrix} a^m_{0,0} & a^m_{1,0} & a^m_{2,0} & b^m_{0,0} & b^m_{1,0} & b^m_{2,0} & a^m_{0,1} & a^m_{1,1} & a^m_{2,1} & b^m_{0,1} & b^m_{1,1} & b^m_{2,1} & \ldots \\ a^m_{0,nez*ner-1} & a^m_{1,nez*ner-1} & a^m_{2,nez*ner-1} & b^m_{0,nez*ner-1} & b^m_{1,nez*ner-1} & b^m_{2,nez*ner-1} & & & & & & & \end{pmatrix}^T \tag{25}$$

A straightforward calculation as described in [1] yields the same expressions for the matrix of the linear system of equations $M_{6p+3i+\alpha,6q+3j+\beta}$ and the right hand side $RS_{6p+3i+\alpha}$ (p, q = $0\ldots nez{*}ner-1$ denote the point in the finite element mesh, i, j = 0, 1 correspond to the cos and sin terms, α, β = $0\ldots2$ denote the component of the vector potential at a mesh point).

6. Application

As a very simple application, Fig. 1 shows a saddle coil inside a metallic cylinder. The saddle coil has a radius of 10 mm, the metallic cylinder has a radius of 100 mm and is 1 mm thick. The relative permeability of the cylinder is 1, its conductivity is 65.000 A/V/mm (copper). At time t = 0 the current in the saddle coil is instantaneously switched off. The field on the axis in the centre of the deflection system follows a settling curve. The settling curve was calculated by two methods. Fig. 2a shows the settling curve determined with the FEM software based on the method described in this paper. For comparison, the settling curve was also calculated using formulas from ref. [7] (see Fig. 2b). For this case a deflection system and a cylinder of infinite length are assumed. The 1/e decrease of 3 ms in the first case is of quite good agreement with the 4 ms in the latter case.

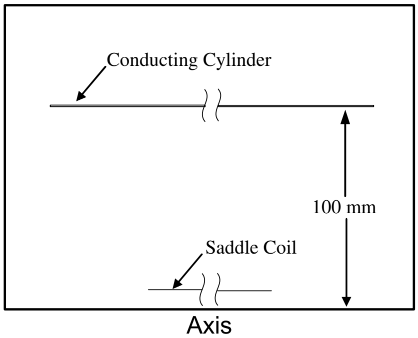

Fig. 1. Magnetic saddle coil surrounded by a metallic cylinder.

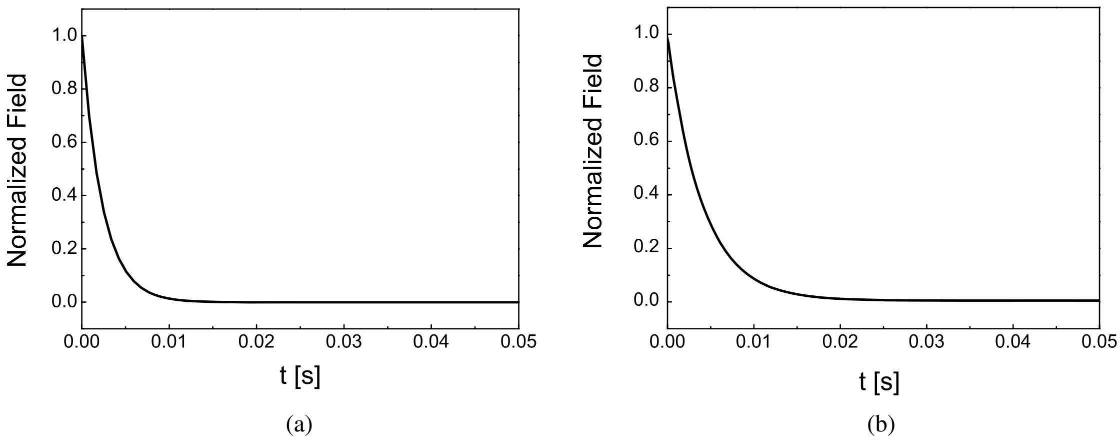

Fig. 2. Settling curves for the magnetic saddle coil surrounded by a metallic cylinder, depicted in Fig. 1.
(a) Settling curve calculated with the FEM software according to the method described in this paper.
(b) Settling curve calculated with formulas from Ref. [7].

For electron beam lithography the time until the field is decreased to one millionth of its initial value is of interest, because the typical main field deflection is on the order of magnitude of 1 mm with a desired accuracy of 1 nm. This can only be achieved with an acceptable settling time if several methods are combined, i.e. applying ferrites as well as featuring the deflection coil with additional coils for (partial) compensation of the outer field [8]. It is obvious that the FEM method can also be applied to this more complicated arrangement. The computation time (Pentium 1 GHz personal computer) for calculating the time-dependant field of a real lens with 100 time steps is approximately 20 h. This is more than two orders of magnitude faster than in the case of a conventional (3D) FEM calculation.

7. Conclusion

The basic formulas for time dependent fields in conductive materials have been developed to be implemented in a FEM-program. The reduction from the 3D-case to a 2D-case gave a dramatic advantage in computing time. (A factor of 100 was achieved in the cases of interest.) The reduction is possible because for eddy current calculations only the first harmonic is of interest in electron optical tools (e.g. electron beam direct write).

Using different sets of materials offers the opportunity to apply the FEM program to final lenses where the pole piece is manufactured from soft iron and a shield of ferrites is used. The FEM software was used to design a new column for electron beam lithography [9].

Acknowledgements

The work for this paper is part of the MEDEA+ Project T207 “65 nm CMOS 300” being handled under the grant number 01M 3147B and is funded by the BMBF (German Ministry for Education and Research).

References

[1] T. Elster, D. Stahl and P. Hahmann, Proceedings of CPO7 (first paper of this series, published in this volume).
[2] E. Munro and H. C. Chu, Optik 60 (1982) 371.
[3] B. Lencova, M. Lenc and K. D. van der Mast, J.Vac.Sc.Technol. B7 (1989) 1846.
[4] M. Kaltenbacher and S. Reitzinger, IEEE Transactions on Magnetics 38 (2002) 513.
[5] R. Beck, Konrad-Zuse-Zentrum für Informationstechnik Berlin, preprint SC 99-40 (1999).
[6] www.exp-math.uni-essen.de/~ajung/diplom/node9.html
[7] H. Kaden, “Wirbelstroeme in der Nachrichtentechnik”, Springer (1950).
[8] K. Kaschlik et al., Exp. Techn. Phys. 28 (1980) 451.
[9] P. Hahmann et al., Resolution Enhancement for Variable-Shaped Beam Writers”, Microelectronic Engineering 84 (2007) 774.